Calibration and performance tests of the Very-Front-End electronics for the CMS electromagnetic calorimeter

J. Blaha, C. Combaret, J. Fay, G. Maurelli

Calibration and performance tests of the Very-Front-End electronics for the CMS electromagnetic calorimeter

J. Blaha[a,1], C. Combaret[a], J. Fay[a], G. Maurelli[a]

on behalf of the CMS ECAL group

[a] IPNL, Université de Lyon, Université Lyon 1, CNRS/IN2P3, Villeurbanne, France

j.blaha@ipnl.in2p3.fr

Abstract

The Very-Front-End electronics processing signals from photodetectors of the CMS electromagnetic calorimeter have been put through an extensive test programme to guarantee functionality and reliability. The final characteristics of the VFE boards designed for the calorimeter barrel and endcaps are presented. The results, which have been also verified during test beam at CERN, confirm the high quality of the boards production and show that the CMS detector specifications are reached.

I. Introduction

On detector electronics of the CMS electromagnetic calorimeter (ECAL) [1], which consist of 75,848 radiation hard scintillating crystals PbWO4, contain almost 16,000 Very-Front-End (VFE) boards that process signals from Avalanche Photodiodes (APDs) in the central barrel region and Vacuum Phototriodes (VPTs) in the forward endcaps regions, respectively. The VFE board was designed in two types: covering a dynamic range up to 50 pC corresponding to an incident particle energy of ~ 1.7 TeV for barrel and 16 pC for energy up to ~ 3.5 TeV for the endcaps. Both types comprise five identical and independent read-out channels. Each channel, processing the signal from one crystal, consists of a Multi-Gain Pre-Amplifier (MGPA), a multi-channel analogue-to-digital convector (ADC) AD41240, and two level adapters LVDS-RX. The VFE ASICs are identical for both types of the board and the different dynamic ranges are set by external electrical components. Schematic drawing of such a channel is displayed in Fig. 1.

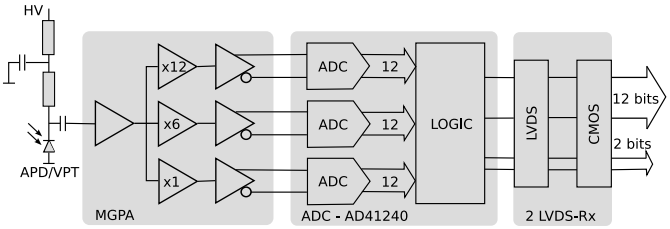

Figure 1: Schematic representation of one channel of the Very-Front-End (VFE) architecture comprising the MGPA, multi-channel ADC AD41240 and two level adapters LVDS-RX.

The MGPA chip [2] contains a pre-amplifier and three parallel gain stages with nominal gain 1, 6, and 12 that shape and amplify the photodetector signal. The three analogue output signals of the MGPA are then digitized in parallel by the multi-channel 40 MHz 12-bit ADC (AD41240) [3]. An ADC internal logic determines whether a gain is saturated and then outputs the data from the highest non-saturated channel. The Low Voltage Differential Signal (LVDS) outputs of the ADC are adapted by two LVDS-RX to the single ended inputs of the front-end (FE) board, which thus receives 12 bit digitalized pulse information and 2 bit identification of the gain. The MGPA chip also includes a test pulse unit with an integrated digital to analogue converter (DAC) programmed via an I^2C interface, which allows the channel functionality to be checked by injecting test charges directly into the input of the pre-amplifier. The pedestal value can be set independently for each gain. In addition, the VFE board also incorporates a Detector Control Unit (DCU) chip for measuring the crystal temperature and, in case of barrel VFE card, also the APD leakage current. All the chips are implemented in 0.25 μm IBM CMOS radiation-hard technology.

To guarantee the functionality and reliability of the VFE electronics, all the VFE boards have to pass an extensive quality and assurance (Q&A) program. The program, which due to its complexity is split among several collaborating institutes (IPN Lyon, ETH Zürich, INFN Torino and University of Cyprus), includes a number of consecutive tests beginning with an optical inspection performed by the manufacturer, followed by a power-on test - the first electrical test that measures voltages, currents and performs a basic functional test, and a burn-in for 72 hours at a temperature of 60 °C, which is finalized by a complete calibration and characterization of each channel. More information about individual steps of the Q&A program can be found elsewhere [4, 5].

II. Calibration and performance tests

The main aim of the calibration and performance test of the VFE card is to fully characterize and verify all the operational parameters of the card and build a calibration database for each card which will serve for the first calibration of all the channels of the CMS ECAL. For this purpose a complete calibration bench has been designed at IPN Lyon. In a 19 inch 6U crate, up to 6 test boards, which serve 6 VFE cards, can be installed and measured at the same time. The test board provides 2.5 V analogue voltage supplying the MGPA and analogue part of the ADC, and 2.5 V digital voltage for digital part of the ADC. An Altera FGPA sends data via a RS 232 bus to the master PC.

[1] Also at the Czech Technical University in Prague

A. Calibration

The calibration procedure includes an absolute calibration of each channel for the three gains in ADC counts versus injected charge in pC, a channel-to-channel relative calibration, gain ratios and linearity studies. An Agilent square pulse generator and an attenuator are used to obtain different voltages that are applied on a calibrated 10 ± 0.01 pF capacitor which gives charges in a range from 0 up to 40 pC and up to 9 pC for the barrel and endcap, respectively. A digital output of the ADC is recorded every 25 ns and an amplitude of the pulse is computed by a 4-parameter analytical function using 5 samples around the maximum value. A pedestal value, which is estimated for each injected charge separately using a set of pre-samples, is subtracted. In order to check the linearity a set of pulses of precise charges are injected into the VFE card and a digital output of the card is recorded over the full dynamic range for all three gains and five channels. Injected charges were chosen to cover the whole range of each gain and to provide sufficient amount of points for the calibration as well as for linearity studies as depicted in Fig. 3.

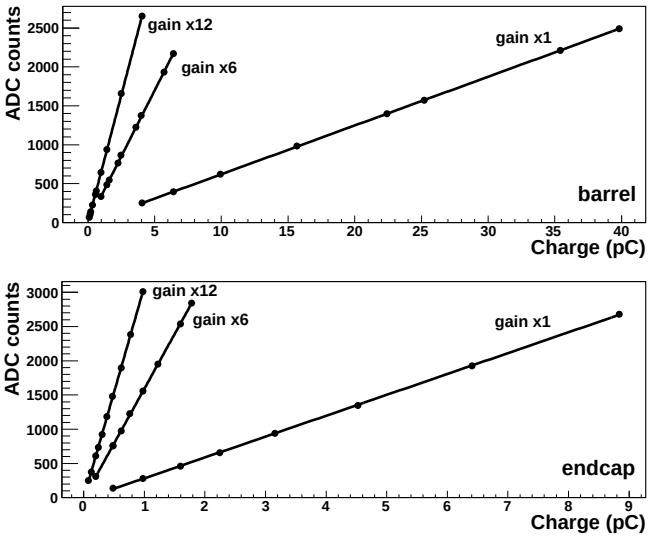

Figure 3: VFE outputs in ADC counts versus injected charge for the barrel (top figure) and endcap VFE (bottom figure) representing calibration curves for the three gains 1, 6, and 12.

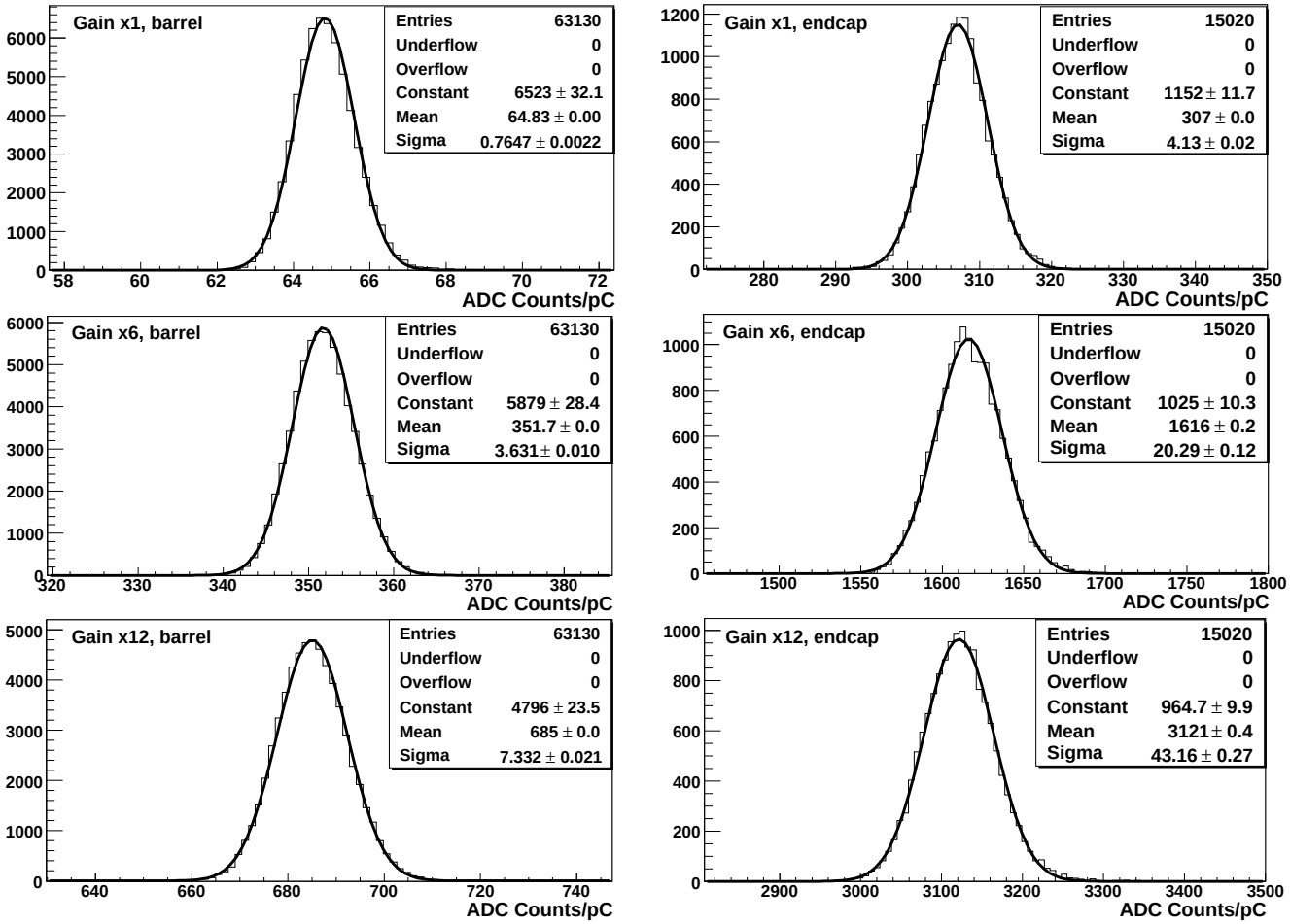

Figure 2: Slope distributions of the injected charges versus pulse height in ADC counts/pC for all the barrel (left figure) and all the endcap VFE (right figure) and the three gains 1, 6, and 12.

A charge of 4 pC for barrel VFE and charges 0.5 and 1 pC for endcap VFE are the only possible charges common for all three gains and which thus allow the gain ratios to be measured directly. In order to suppress instrumentation effects from the test boards of the calibration system and variation during the long period of calibration of more than two years, an intercalibration between channels is applied. Since a pulse height temperature dependency and slope dependency of -0.2%/°C were observed, all the calibration measurements are performed in a temperature stabilized room (18±0.3°C).

Measurements of the calibration curves, shown for one channel in Fig. 3, have been completed for all VFE cards needed for barrel and endcaps. Parameters of a linear least square fit of the calibration curve fully describe the main properties of each gain channel. Average values of the slopes, which represent the gains, measured in ADC counts per pC over all calibrated channels are listed together with the corresponding dispersions in Tab. 1. Very small differences (σ/mean $\sim 1\%$) among measured channels prove the high quality and homogeneity in the VFE board production. Slope distributions of the injected charge versus pulse height in ADC counts/pC for all the barrel and endcap VFE card for three gains 1, 6, and 12 are displayed in Fig. 2.

	Barrel		Endcap	
Gain	**Slope**	**σ/mean (%)**	**Slope**	**σ/mean (%)**
1	64.83	1.18	307	1.35
6	351.7	1.03	1616	1.26
12	685	1.07	3121	1.38

Table 1: Mean value of the slopes (ADC count/pC) of the injected charges versus pulse height and its dispersion (%) for all the barrel and endcap VFE cards for three gains 1, 6, and 12.

B. *Gain ratio*

The laboratory gain ratio is determined as the ratio of slopes of the calibration curve between the gains. Mean values and corresponding dispersions over all the measured channels are summarized in Tab. 2 for the barrel as well as for endcap VFEs. The gain ratio values presented in Tab. 2 show small dispersion among the channels.

	Barrel		Endcap	
Ratio	**Mean**	**σ/mean (%)**	**Mean**	**σ/mean (%)**
12/1	10.74	1.001	10.84	1.284
12/6	1.943	0.87	1.951	1.121
6/1	5.527	0.887	5.559	1.175

Table 2: Mean values of the gain ratios and corresponding dispersions for all the barrel and endcap VFE cards.

Precision of knowledge of the gain ratio plays a very important role for higher or extremely high energies where switching to gain 6 or 1 occurs. For this purpose, it was necessary to develop an alternative technique for the gain ratio determination which could be used as an in situ method during CMS ECAL operations. Hence, the MGPA test pulse unit was used for gain ratio computation. By this unit it is possible to inject a test charge directly into the input of the MGPA amplifier. Because the gain path can be forced to a particular choice by stopping one or more ADC gains, it is possible for the same injected charge to produce signals from different gain stages. Thus a ratio of the reconstructed signal amplitudes is equal to the gain ratio. The gain ratio delivered by the test pulse and extracted from the slopes were compared and it was found that both methods give comparative results, well-correlated among channels, but with a small systematic shift which can be due to different circuitry for the injected charge.

Another technique for in situ gain ratio determination uses the ECAL laser monitoring system [6], which monitors variations in the light transmission of the crystals due to radiation during LHC operation. The gain ratio is measured by forcing gain changes for a fixed laser light pulse. The gain ratio measured by the test pulse with a charge of 4 pC and by monitoring laser system using an infrared light, were compared and it was found that both methods give comparative results, well-correlated among channels as seen in Fig. 4.

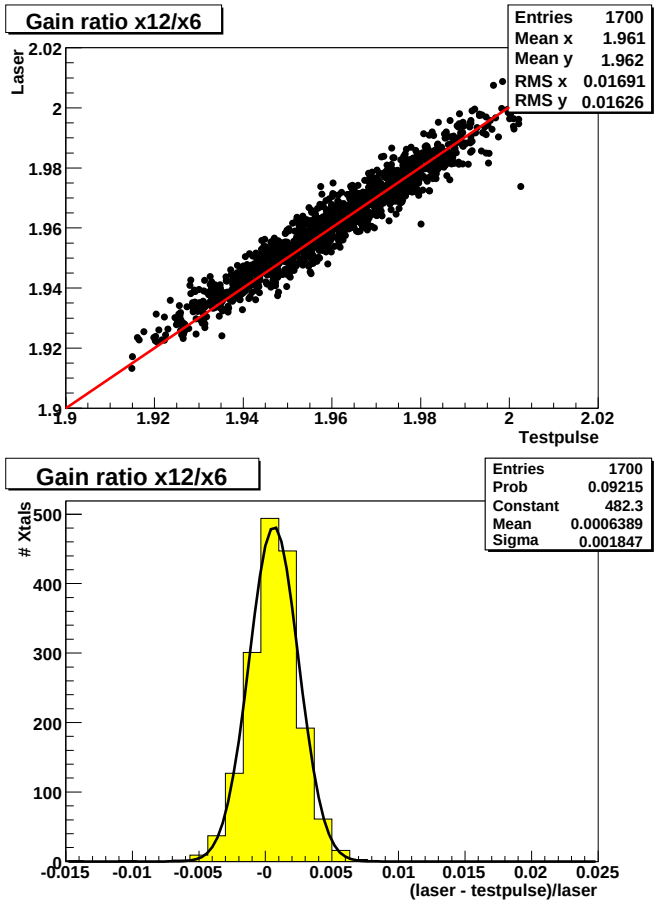

Figure 4: Correlation (top) and difference (bottom) between gain ratio 12/6 measured by the test pulse and laser on a barrel supermodule.

In order to verify the reliability of the gain ratio measurement with the test pulse, an electron beam of 120 GeV was used to determine gain ratio in data taking conditions. The results (see Fig. 5) have confirmed that gain ratios obtained by the test pulses can be measured with sufficient precision and stability and thus could be used as a reliable method for the gain ratio determination for the whole CMS ECAL.

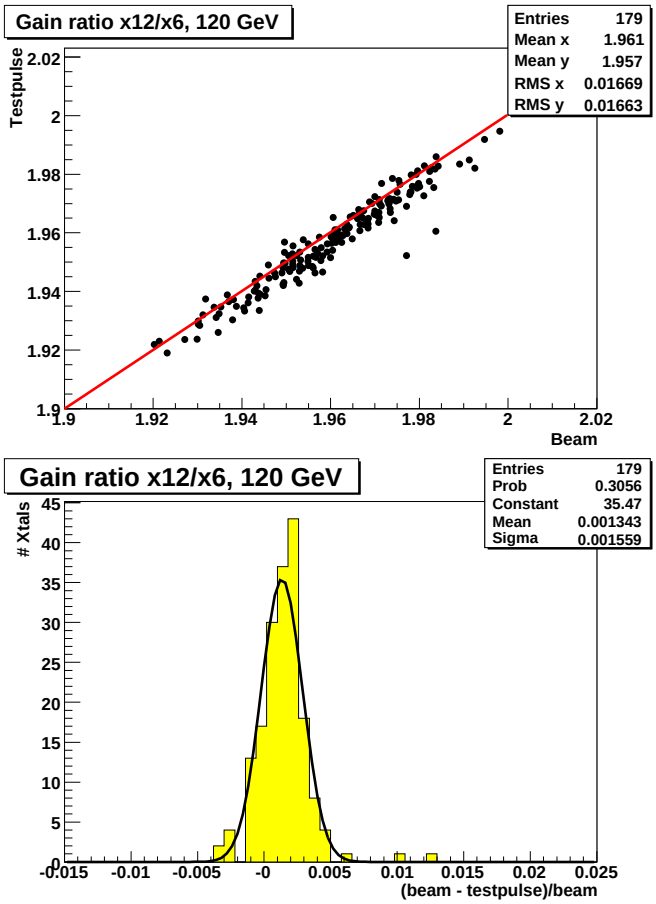

Figure 5: Correlation (left) and difference (right) between gain ratio 12/6 measured by the MGPA test pulse and with an electron beam of 120 GeV at CERN for 179 channels.

C. Linearity

Tests of linearity were evaluated by help of the coefficient of determination r^2 delivered from the linear fit of the calibration curve. The coefficient is better than 99.99% for all the channels for barrel VFE cards. Since the dynamic range is different for the endcap and also because of a lower precision in the charge determination for small charges, the coefficient is greater than 99.98% for the endcap VFE cards. In both cases, only very small non-linearity was found.

D. Pedestal and electronic noise

Pedestal is the electronic baseline on which an electrical signal is carried. Its value is programmable using a simple DAC circuit internal to the MGPA which is controlled externally by an I^2C interface. Correct functionality of the pedestal setting was verified in two different but complementary ways. In the first case, special pedestal measurements for each gain were performed. The DAC value is varied from 0 up to 100 and corresponding pedestal value is recorded. Fig.6 shows DAC values versus pedestal for one VFE card. After setting the pedestal fluctuation was evaluated from dedicated pedestal runs when no charge was injected. In addition, the pedestal was also computed from pre-samples taken prior to the injected charge. These tests were performed for each gain separately.

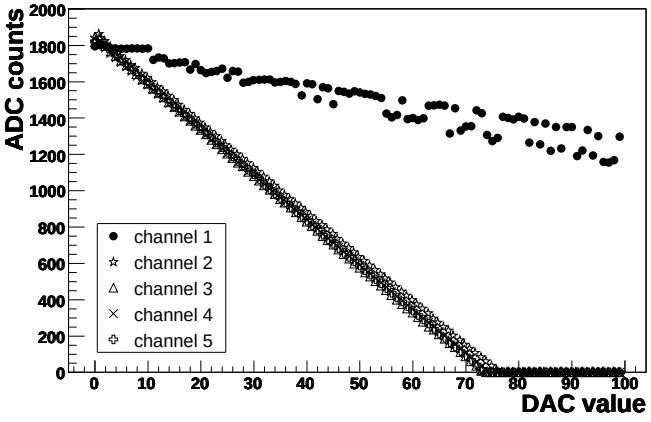

Figure 6: DAC value versus pedestal for five channels of the barrel VFE card, gain 1. The channel 1 does not work correctly, hence this VFE card has been rejected.

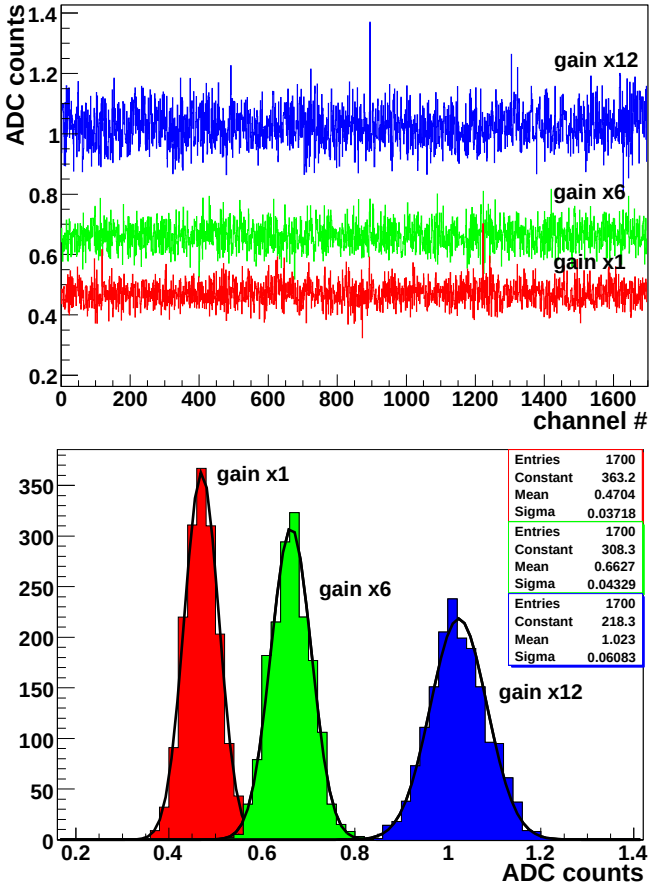

Figure 7: Electronic noise in ADC counts versus channel number (top) and its distribution (bottom) for a barrel supermodule (1,700 crystals).

The pedestal runs were also used for an estimation of the electronic noise as the rms of the pedestal distribution. The noise values on the calibration bench are greater than measured in ECAL which is due to the important contribution from calibration system itself. VFE cards for which the pedestal could not be set correctly or the rms noise was greater than 10 σ of the noise distribution for all measured channels were rejected.

In situ electronic noise was measured during the test beam on fully assembled supermodules by applying the amplitude re-

construction weight method [7] on the pedestal runs. A typical mean value of the electronic noise for a single channel over an entire barrel supermodule (1,700 channels) is around 1 ADC count (∼37 MeV) for gain 12. This value includes all contributions to the noise over the whole ECAL electronics chain. In Fig. 7 the electronics noise is plotted for all three gains for one supermodule, showing that the dispersion over the channels is very small.

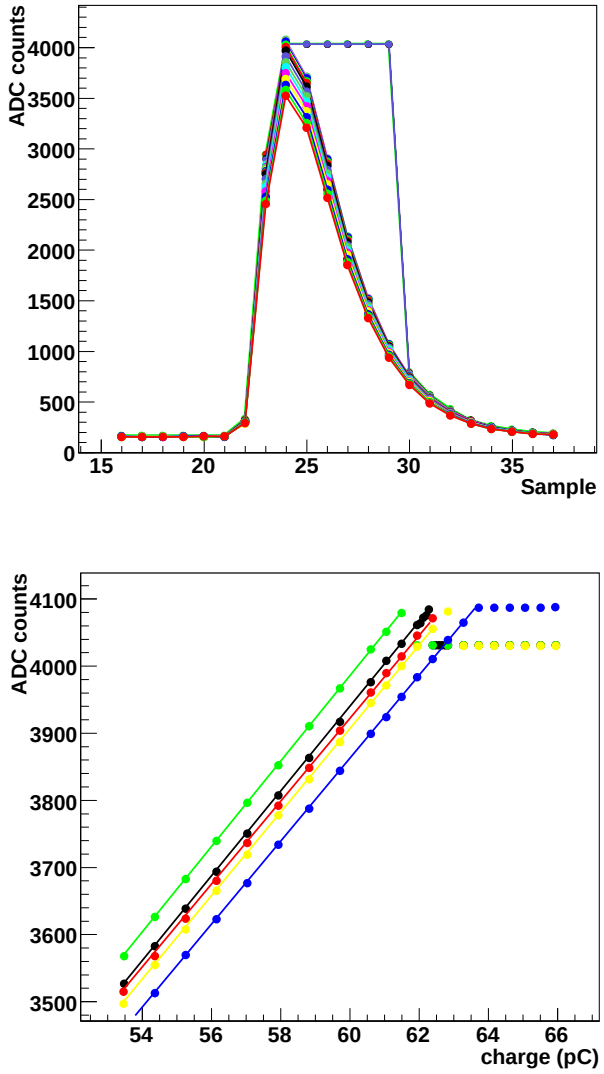

Figure 8: ADC output for different injected charge in a single channel (top) and linearity plot for five channels of the barrel VFE board (bottom).

E. Electronic saturation

The gain 1 saturation effect was studied on the barrel VFE board by applying injected charges up to 66 pC (above the specification and corresponding to $>$ 2 TeV energy). It was found that the ADC saturates before the MGPA, which is linear up to levels larger than 3,900 ADC counts. If saturation occurs the ADC returns five consecutive samples with same value as can be seen in Fig. 8 top. Fig. 8 (bottom) shows that once the saturation is reached, it does not change with increasing value of the injected charge. It was also proven that saturation does not affect the timing corresponding to the maximum of the signal collection needed for L1 triggering and thus does not distort the LHC bunch crossing identification.

F. Slow control

Other relevant tests, such as the calibration of leakage current measurements of the APDs and temperature read-out channel on its complete dynamic range are also performed. The DCU chip placed on the VFE card collects data and sends them to the data acquisition system via the I^2C interface. For the temperature read-out channel, which is used for each 10^{th} crystal, the test board uses a digital potentiometer that changes its value to simulate a temperature variation of the crystals. The stability of the leakage current is tested using a current source which simulates a variation of the leakage current in a range between 0 – 200 nA to the input of the VFE.

III. Summary and Conclusion

The test program for all the 12,240 barrel and the ∼3,000 endcap VFE boards has been completed. The dispersion in the gains is found to be small (∼1%). Noise, linearity and gain ratios are complying with the CMS detector specifications. Only around 2 % of them failed the test criteria and have been rejected, the rest have been assembled into barrel supermodules and soon will be also into endcap supercrystals. Results are registered in a database and can be used for a first intercalibration of the ECAL. The results obtained during the Q&A program have been verified in summer 2006 and 2007, when several fully equipped supermodules and supercrystals were tested and calibrated with high energy electrons.

References

[1] CMS Collaboration, CMS Physics: Technical Design Report – Detector performance and software, Vol. 1, Technical Design Report CMS, CERN/LHCC 2006-001, 2006

[2] M. Raymond *et al.*, The MGPA Electromagnetic Calorimeter Readout Chip for CMS, IEEE Trans. Nucl. Sci., Vol. 52, 2005, pp 756–763

[3] G. Minderico *et al.*, A CMOS Low Power, Quad Channel, 12 bit, 40MS/s Pipelined ADC for Applications in Particle Physics Calorimetry, 9^{th} Workshop on Electronics for LHC Experiments, 2003, pp 88–91

[4] J. Blaha *et al.*, Calibration of the very-front-end electronics for the electromagnetic calorimeter of the CMS experiment, Czech. J. Phys., Vol. 56, 2006, pp 879–881

[5] A. Nardulli *et al.*, Performance of CMS ECAL Very Front End Electronics, 12^{th} Workshop on Electronics for LHC Experiments, 2006, pp 174–178

[6] D. Bailleux *et al.*, Performance of the Monitoring Light Source for the CMS Lead Tungstate Crystal Calorimeter, IEEE Trans. Nucl. Sci., Vol.52, 2005, pp 1123–1130

[7] R. Brunelière and A. Zabi: Reconstruction of the signal amplitude of the CMS electromagnetic calorimeter, CERN CMS NOTE 2006/037, 2006